
EUV IMAGING SPECTROMETER

Hinode

EIS SOFTWARE NOTE No. 26

Version 1.0

27 January 2023

Creating synthetic EIS rasters from SDO/AIA data

Peter Young
NASA Goddard Space Flight Center
Greenbelt, MD 20771
U.S.A.

1. Introduction

This document describes how to make a synthetic EIS raster from a sequence of images from the Atmospheric Imaging Assembly (AIA) on board the Solar Dynamics Observatory. The routine can reproduce both spatial raster maps and sit-and-stare time series data.

2. Procedure

- Determine which EIS emission line and which AIA channel to use. For example, Fe XII 195.12 Å and AIA 193 Å, or He II 256.32 Å and AIA 304 Å.
- Download a sequence of cutout images in the AIA filter from the Joint Science Operations Center (JSOC: <http://jsoc.stanford.edu/>). The images should be larger than the EIS field of view and the sequence should extend at least as long as the EIS observation.
- Create an EIS image map using the selected line.
- Make an initial guess for the spatial offset of the two instruments.
- Run the routine `aia_make_eis_raster` for a range of x and y values around the initial offset value.
- Compare the EIS image and the synthetic EIS image (obtained from the AIA cutouts) and determine which of the different spatial offset values gives the best agreement by, for example, overlaying the images.

3. The `aia_make_eis_raster` routine

This routine is available in a GitHub repository, which can be obtained by doing:

```
> git clone https://github.com/pryoung/sdo-idl.git
```

If the AIA cutout filenames are stored in `aia_filenames`, the EIS windata structure for the selected line is stored in `wd`, and the EIS image map (see above) is stored in `eis_map`, then the call is:

```
IDL> syn_map=aia_make_eis_raster(aia_filenames,wd,eis_map=eis_map)
```

This routine builds the synthetic EIS map as follows:

1. The x and y coordinates for each EIS pixel are obtained from the windata structure, and corrected for the values from `eis_aia_offsets`, and for the optional offset specified to `aia_make_eis_raster` (both these offsets are added to the windata values).
2. Each AIA cutout is read into an IDL map, and the images are convolved with a 2D Gaussian of width 3 arcsec to mimic the EIS spatial resolution.
3. For each EIS exposure, the routine finds the AIA image or images that lie within the time period $[t_0, t_1]$ where t_0 is the start time of the EIS exposure minus 2 seconds, and t_1 is the end time of the EIS exposure plus 2 seconds.
4. For each of the AIA images corresponding to the EIS exposure,
 - a. the image is rebinned in the y-direction to 1 arcsec pixels (to match EIS);
 - b. the AIA image columns that are within $\pm dx$ of the center of the EIS slit are placed in the output image column corresponding to the EIS exposure, where dx is the slit width divided by 2 plus 0.5";
 - c. the final output image column is then divided by the number of AIA columns that were used to create the column.
5. The bottom pixel of the EIS map is then matched against the synthetic map, and the synthetic map is trimmed in the y direction to match the size of the EIS map.

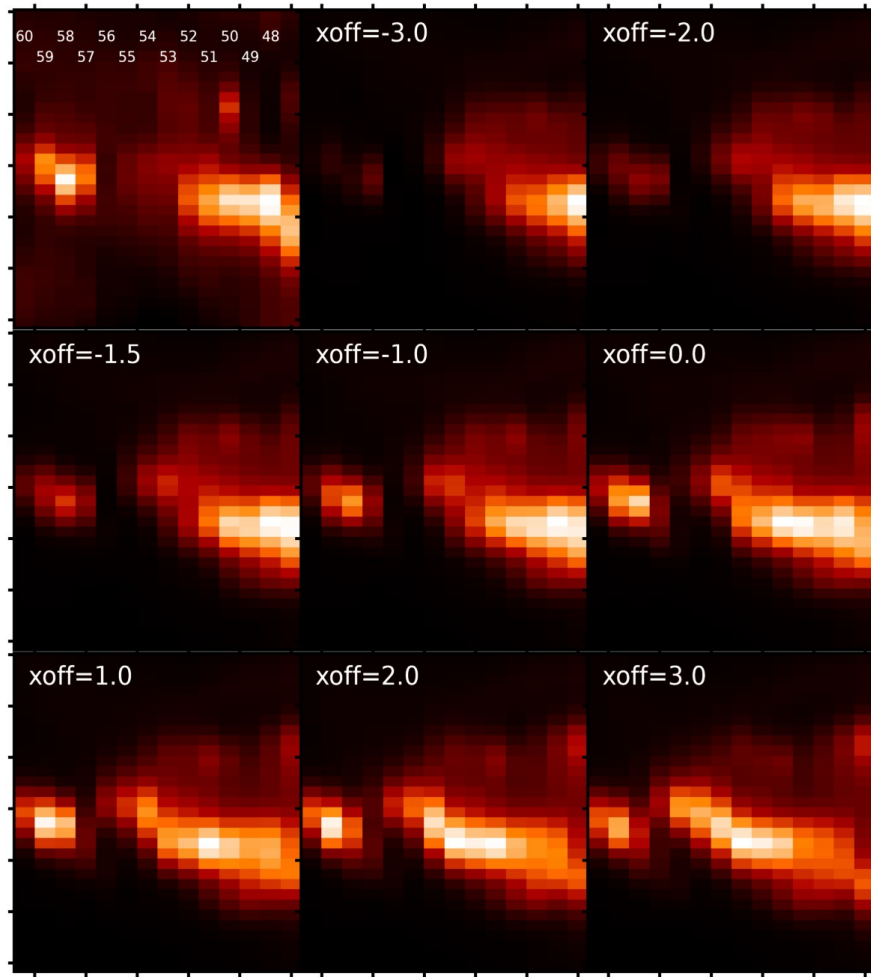


Figure 1. The top-left image shows the EIS Fe XIV 274.20 raster image. The remaining eight panels are synthetic rasters formed from AIA 94 Å images (see main text).

The output map has exactly the same size and spatial scale as the EIS map.

4. Example: a flare raster from 9 March 2012

An M-class flare was caught in an Atlas_30 raster taken between 03:09 and 03:41 UT on 9 March 2012. This flare was analyzed by Doschek et al. (2013, ApJ).

The O IV lines between 270 and 280 Å were bright in a compact region at the left-hand side of the raster. In order to understand the spatial relationship of this region to the evolution of the flare as a whole, it was necessary to construct a synthetic EIS raster from the AIA data.

The emission was clearly related to flare ribbons, and it is known that flare ribbons look fairly similar in a range of coronal lines. Many of the AIA filter images were saturated during the flare, but the 94 Å images were unsaturated hence these were used. AIA 94 Å cutout images matching the EIS observations were downloaded from the JSOC.

The EIS Fe XIV 274.20 Å line was chosen as it was close in wavelength to the O IV lines, was unsaturated and was close enough in temperature of AIA 94 Å (dominated by Fe XVIII) that images could be expected to be similar.

Figure 1 shows the results from using `aia_make_eis_raster` for a set of x-offset values (indicated on the Figure panels). The top-left image is the Fe XIV image and each image column is numbered by their exposure numbers (there are 60 exposures in the raster, and only a sub-region of the original raster is shown). The remaining images are raster images derived from the AIA 94 Å cutouts. The y-offset is fixed at -4''.

In assessing these images, our main criterion is that the brightening on the left side of the images should be reproduced reasonably well. It is clear that offsets of $x < -2.0$ do not work. The simulated slit of AIA is too far to the left of the brightening to give a useful signal. Similarly, offsets of $x > 0.0$ do not work as the brightening at the left has a peak intensity in exposure 59 when it should be exposure 58. The intensity distribution of the extended feature to the right (exposures 48 to 55) is also not well reproduced.

Considering the morphology of the brightening, offset -1.5 best reproduces the EIS image. However, the brightening is somewhat weaker compared to the emission on the right side of the image. The contrast is better for offsets -1.0 and 0.0, but the emission in exposure 57 is weaker than in the EIS image when compared to exposure 58. Since the purpose of the O IV analysis was to study the brightening, then the offset of -1.5 was selected.

5. Example: a sit-and-stare flare dataset from 2-Apr-2022

A sit-and-stare study was run near an active region when an M-class flare occurred. The evolution of the erupting filament was captured in the EIS observation between 13:05 UT and 14:06 UT, and there were 225 exposures.

For sit-and-stare data, the image that is created has time and solar-y axes. The routine `eis_make_image` creates an IDL map from the EIS data, and is not intended for use with sit-and-stare data, however it can still be used in the present case.

The image produced by `eis_make_image` correctly has time evolution from left-to-right, but the map has spatial coordinates in the x-direction. The coordinates are such that the center of image corresponds to the true x-cen value of the data-set. The x-scale is set to the slit width (2'' in the present case).

When constructing the synthetic image, `aia_make_eis_raster` uses the `solar_x` tag of the `windata` structure in order to identify which AIA image columns should become part of the synthetic EIS image. The coordinates of the EIS map are not used. Since the `solar_x` tag has the correct x-coordinates, then this step works correctly.

For this dataset, He II 256.32 Å was used for EIS and the 304 Å channel (dominated by He II) for AIA. Since there were strong blueshifts associated with the erupting filament, the EIS map was constructed with the following call:

```
IDL> eis_make_image,file,256.20,map256,/map,wpix=12
```

That is, the central wavelength was chosen in the blue wing (at -140 km/s) and +/- 12 pixels either side of this wavelength were averaged (wpix input), which ensures that all the emission from the blue wing and the line's rest component are included.

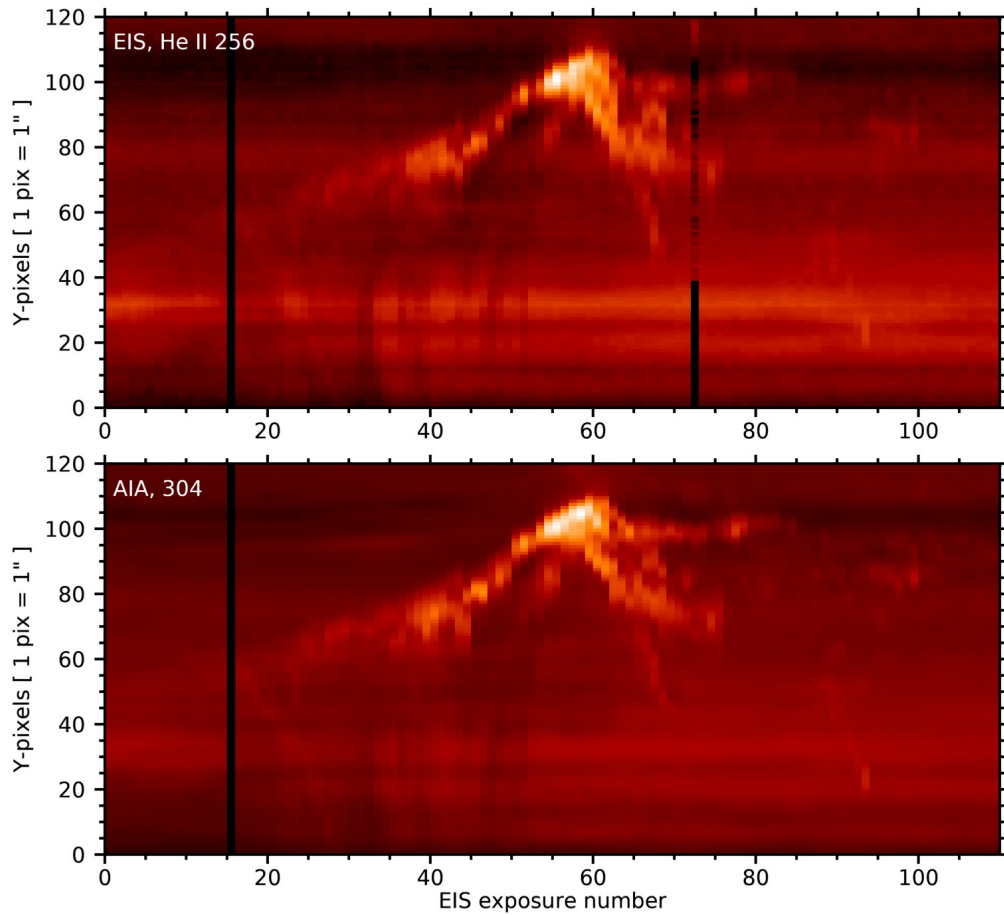


Figure 2. The top images shows the He II 256 image from EIS, and the bottom image shows the synthetic EIS image derived from AIA 304.

Figure 2 gives a comparison of the EIS He II 256 Å image from the dataset to the synthetic EIS image derived from AIA 304 Å. An x-offset of 6'' and a y-offset of 15'' were used to generate the AIA image. The procedure did an excellent job of reproducing the EIS features, including the faint, compact ejecta around exposures 90 to 100.

6. Limitations

The AIA images are corrected for the SDO roll angle. The EIS images are assumed to be aligned north-south, yet the instrument has a known and variable roll angle that was measured by Pelouze et al. (2019, Sol. Phys.). This will affect the alignment of large raster images, but for small rasters or sit-and-stare data with a small y-range the effect will likely be small.

7. Python software: eis_pointing (G. Pelouze)

Pelouze et al. (2019, Sol. Phys.) presented Python software for performing coalignment of AIA and EIS. The software uses Fe XII 195.12 Å and AIA 193 data for the alignment, and jitter and roll are corrected in addition to image translation. The AIA images are obtained at 1 minute cadence, which may not be sufficient for flare data such as those shown in the present document.

The software is available on GitHub in https://github.com/gpelouze/eis_pointing, and the calling sequence is as follows:

```
> compute_eis_pointing -c16 eis_10_20140810_042212
```

See the online documentation for more details.

Update history

Version 1.0, 27-Jan-2023 – first version created.